

## Aryl Bridged 1-Hydroxypyridin-2-one: Effect of the Bridge on the Eu(III) Sensitization Process

Anthony D'Aléo, Evan G. Moore, Géza Szigethy, Jide Xu, and Kenneth N. Raymond\*

*Chemical Sciences Division, Lawrence Berkeley National Laboratories, Berkeley, California 94720 and Department of Chemistry, University of California, Berkeley, California 94720-1460*

Received June 17, 2009

The efficiency of Eu<sup>3+</sup> luminescence by energy transfer from an antenna ligand can be strongly dependent on the metal ion coordination geometry. The geometric component of the Eu(III) sensitization has been probed using series of tetradentate 1,2-HOPO derivatives that are connected by bridges of varying length and geometry. The ligands are *N,N'*-(1,2-phenylene)bis(1-hydroxy-6-oxo-1,6-dihydropyridine-2-carboxamide) for the ligand (L<sup>1</sup>), 1-hydroxy-*N*-(2-(1-hydroxy-6-oxo-1,6-dihydropyridine-2-carboxamido)benzyl)-6-oxo-1,6-dihydropyridine-2-carboxamide (L<sup>2</sup>) and *N,N'*-(1,2-phenylenebis(methylene))bis(1-hydroxy-6-oxo-1,6-dihydropyridine-2-carboxamide) (L<sup>3</sup>). Spectroscopic characterization of both the Gd(III) and the Eu(III) metal complexes, time-dependent density functional theory (TD-DFT) analysis of model compounds and evaluation of the kinetic parameters for the europium emission were completed. Some striking differences were observed in the luminescence quantum yield by altering the bridging unit. The [Eu(L<sup>2</sup>)<sub>2</sub>]<sup>−</sup> derivative shows efficient sensitization coupled with good metal centered emission. For [Eu(L<sup>3</sup>)<sub>2</sub>]<sup>−</sup>, the large quenching of the luminescence quantum yield compared to [Eu(L<sup>2</sup>)<sub>2</sub>]<sup>−</sup> is primarily a result of one inner sphere water molecule bound to the europium cation while for [Eu(L<sup>1</sup>)<sub>2</sub>]<sup>−</sup>, the low luminescence quantum yield can be attributed to inefficient sensitization of the europium ion.

### Introduction

Luminescent lanthanide complexes have attracted much recent attention because of their use in a wide variety of applications such as biofluoroimmunoassay,<sup>1,2</sup> as sensors,<sup>3–7</sup>

in light emitting diodes,<sup>8–10</sup> and as waveguide amplifiers for lasers.<sup>11–18</sup> In most cases, these complexes consist of a lanthanide ion attached to a chelating chromophore which acts as a sensitizer, transferring its excitation energy to the lanthanide ion, and protecting the ion from water coordination. The presence of the chromophore overcomes the limitation of an intrinsically small molar absorption coefficient ( $\epsilon$ ) for the metal by using a strongly absorbing organic ligand (*antenna effect*) by thus increasing the brightness (defined as the product of the luminescence quantum yield and of the molar absorption coefficient). The luminescence lifetimes of the lanthanide ions, which are highly sensitive to the local environment and especially to quenching by OH vibrations are maintained by keeping water molecules out of the inner coordination sphere. The unique properties of these ions include line like emission (going from the visible to the Near Infra-Red [NIR] by changing the lanthanide used), very long lifetimes (from the millisecond or submillisecond range for the visible emitters to the microsecond or submicrosecond

\*To whom correspondence should be addressed. E-mail: raymond@socrates.berkeley.edu.

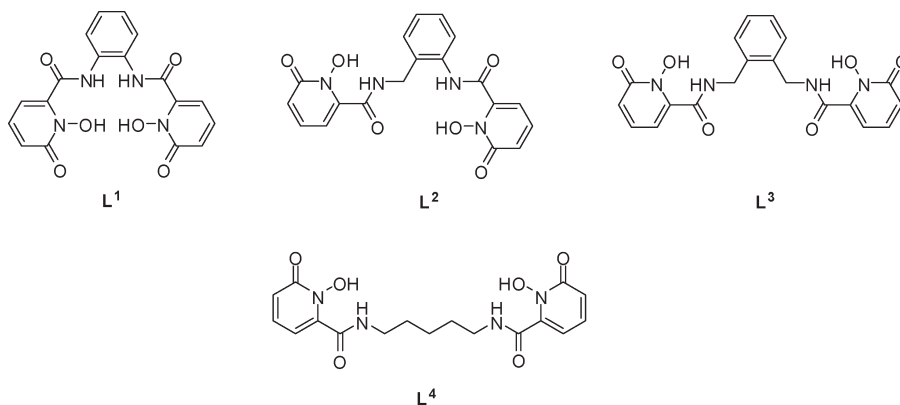
- (1) Handl, H. L.; Gillies, R. J. *Life Sci.* **2005**, *77*, 361–371.
- (2) Petoud, S.; Cohen, S. M.; Bünzli, J.-C. G.; Raymond, K. N. *J. Am. Chem. Soc.* **2003**, *125*, 13324–13325.
- (3) Song, B.; Wang, G.; Tan, M.; Yuan, J. J. *Am. Chem. Soc.* **2006**, *128*, 13442–13450.
- (4) Borisov, S. M.; Wolbeis, O. S. *Anal. Chem.* **2006**, *78*, 5094–5101.
- (5) Stich, M. I.; Nagl, S.; Wolbeis, O. S.; Henne, U.; Schaeferling, M. *Adv. Funct. Mater.* **2008**, *18*, 1399–1406.
- (6) Parker, D. *Coord. Chem. Rev.* **2000**, *205*, 109–130.
- (7) Tremblay, M. S.; Halim, M.; Sames, D. *J. Am. Chem. Soc.* **2007**, *129*, 7570–7577.
- (8) Kido, J.; Okamoto, Y. *Chem. Rev.* **2002**, *102*, 2357–2368.
- (9) Kang, T.-S.; Harrison, B. S.; Foley, T. J.; Knefely, A. S.; Boncella, J. M.; Reynolds, J. R.; Schanze, K. S. *Adv. Mater.* **2003**, *15*(13), 1093–1097.
- (10) De Bettencourt-Dias, A. *Dalton Trans.* **2007**, 2229–2241.
- (11) Kuriki, K.; Koike, Y.; Okamoto, Y. *Chem. Rev.* **2002**, *102*, 2347–2356.
- (12) Kim, H. K.; Roh, S. G.; Hong, K.-S.; Ka, J.-W.; Baek, N. S.; Oh, J. B.; Nah, M. K.; Cha, Y. H.; Ko, J. *Macromol. Res.* **2003**, *11*(3), 133–145.
- (13) Julian-Lopez, B.; Planelles-Arago, J.; Cordoncillo, E.; Viana, B.; Sanchez, C. J. *Mater. Chem.* **2008**, *18*(1), 23–40.
- (14) Weber, J. K. R.; Felten, J. J.; Cho, B.; Nordine, P. C. *Nature* **1998**, *393*, 769–771.
- (15) Slooff, L. H.; Polman, A.; Klink, S. I.; Hebbink, G. A.; Grave, L.; van Veggel, C. J. M.; Reinhoudt, D. N.; Hofstraat, J. W. *Opt. Mater.* **2000**, *14*, 101–107.

(16) Slooff, L. H.; Blaaderen, A. V.; Polman, A.; Hebbink, G. A.; Klink, S. I.; van Veggel, C. J. M.; Reinhoudt, D. N.; Hofstraat, J. W. *J. Appl. Phys.* **2002**, *91*, 3955–3980.

(17) Moynihan, S.; Van Deun, R.; Binnemans, K.; Krueger, J.; von Papen, G.; Kewell, A.; Crean, G.; Redmond, G. *Opt. Mater.* **2007**, *29*, 1798–1808.

(18) Escribano, P.; Julian-Lopez, B.; Planelles-Arago, J.; Cordoncillo, E.; Viana, B.; Sanchez, C. J. *Mater. Chem.* **2008**, *18*, 23–40.

Chart 1. Structures of the 1,2-HOPO Ligands Investigated



range for the NIR emitters) and the relative insensitivity of their emission to the presence of dioxygen.<sup>19,20</sup>

Despite extensive research, the optimization of the energy transfer for the sensitization of the lanthanide ion by exciting complexed chromophores is still not fully understood. In this regard, the europium ion is an interesting probe since Beeby et al.<sup>21</sup> and Verhoeven et al.<sup>22</sup> have shown that the steady state luminescence spectrum and the luminescence lifetime of the europium ion can be used to evaluate the efficiency of the sensitization process.

Herein, we report the synthesis and optical studies of some aryl bridged 1-hydroxypyridin-2-one (1,2-HOPO) derivatives. The use of an aryl unit as a bridge<sup>23</sup> (compared to aliphatic versions previously published<sup>24,25</sup>) has been shown recently to not significantly affect the triplet excited state energy, but has a strong effect on the luminescence quantum yield ranging from about 21% for aliphatic bridged derivatives to 6% for [Eu(L<sup>1</sup>)<sub>2</sub>]<sup>-</sup> in aqueous solution at pH = 7.4. Furthermore, these types of 1,2-HOPO containing ligands have been previously shown to be efficient europium sensitizers and form highly stable complexes.<sup>24,25</sup> In particular, the high thermodynamic stability of the complexes in aqueous solution allows measurements at  $\mu$ M and even nM concentrations without evidence of hydrolysis or dissociation. Following these observations, we have prepared two additional 1,2-HOPO derivatives containing a phenyl with one (L<sup>2</sup>) or two (L<sup>3</sup>) methylene group(s) in the ortho positions to isolate the phenyl group from one or both 1,2-HOPO units (Chart 1) and compared these systems to the already reported [Eu(L<sup>1</sup>)<sub>2</sub>]<sup>-</sup> complex.<sup>23</sup> To better understand the differences between these systems, the photophysical data were analyzed using the methods described by Beeby<sup>21</sup> and Verhoeven<sup>22</sup> in three different solvents: two protic solvents (buffered water at pH = 7.4 and methanol) and an aprotic solvent (dimethylsulfoxide, DMSO).

## Experimental Section

**General Procedures.** 2-Aminobenzylamine was purchased from Sigma-Aldrich while  $\alpha,\alpha'$ -diamino-*o*-xylene was synthesized as described elsewhere<sup>26</sup> as were L<sup>1</sup> and L<sup>4</sup> and their Gd and Eu complexes.<sup>23–25</sup> Thin-layer chromatography (TLC) was performed using precoated Kieselgel 60 F254 plates. Flash chromatography was performed using EM Science Silica Gel 60 (230–400 mesh). NMR spectra were obtained using either Bruker AM-300 or DRX-500 spectrometers operating at 300 (75) MHz and 500 (125) MHz for <sup>1</sup>H (or <sup>13</sup>C), respectively. <sup>1</sup>H (or <sup>13</sup>C) chemical shifts are reported in parts per million relative to the solvent resonances, taken as  $\delta$  7.26 ( $\delta$  77.0) and  $\delta$  2.49 ( $\delta$  39.5), respectively, for CDCl<sub>3</sub> and (CD<sub>3</sub>)<sub>2</sub>SO (DMSO-*d*<sub>6</sub>) while coupling constants (*J*) are reported in hertz. The following standard abbreviations are used for characterization of <sup>1</sup>H NMR signals: s = singlet, d = doublet, t = triplet, m = multiplet, dd = doublet of doublets. Fast-atom bombardment mass spectra (FAB<sup>+</sup> MS) were obtained using 3-nitrobenzyl alcohol (NBA) or thioglycerol/glycerol (TG/G) as the matrix. Elemental analyses were performed by the Microanalytical Laboratory, University of California, Berkeley, CA.

**Synthesis. General Method for the Preparation of Benzyl Protected 1,2-HOPOBn Derivatives.** Over a 1 h period, a solution of 1,2-HOPOBn acid chloride<sup>27</sup> (2.4 equiv) in dry dichloromethane (35 mL) was added dropwise to a mixture of the appropriate diamine derivative (1 equiv) and 30% potassium carbonate solution (5 mL) in dichloromethane (20 mL) with vigorous stirring and external cooling by means of an ice bath. The mixtures were warmed to room temperature with stirring, until TLC indicated the reactions were complete. The organic phase was separated, and the crude products were loaded on a flash silica column. Elution with 2–4% methanol in dichloromethane allowed for facile separation of the benzyl-protected precursors, which were all pale yellow oils that solidify upon standing.

**2-Aminomethylaniline-1,2-HOPOBn ((L<sup>2</sup>Bn)).** Yield: 85%; <sup>1</sup>H NMR (500 MHz, CDCl<sub>3</sub>):  $\delta$  4.32 (d, 2H), 4.79 (s, 2H), 5.37 (s, 2H), 6.33 (dd, <sup>3</sup>*J* = 7.0 Hz, <sup>4</sup>*J* = 1.5 Hz, 1H), 6.40 (m, 2H), 6.69 (dd, <sup>3</sup>*J* = 9.0 Hz, <sup>4</sup>*J* = 1.5 Hz, 1H), 6.84 (d, <sup>3</sup>*J* = 7.0 Hz, 2H), 7.08 (m, 3H), 7.19–7.31 (m, 6H), 7.38 (d, <sup>3</sup>*J* = 7.5 Hz, 1H), 7.44 (m, 3H), 8.01 (d, <sup>3</sup>*J* = 8.0 Hz, 1H), 8.26 (s, 1H), 10.29 (s, 1H); <sup>13</sup>C NMR (125 MHz, CDCl<sub>3</sub>):  $\delta$  39.7, 78.3, 78.8, 104.7, 106.4, 122.7, 123.0, 124.2, 125.9, 127.9, 128.3, 128.6, 129.3, 129.6, 129.8, 130.8, 132.1, 132.9, 134.5, 137.7, 137.8, 141.3, 143.0, 157.9, 158.1, 158.9, 160.4; FAB<sup>+</sup> MS: *m/z*: 577 (MH<sup>+</sup>) (calcd: 913.07).

***o*-Aminomethyl-benzylamine-1,2-HOPOBn ((L<sup>3</sup>Bn)).** Yield: 83%; <sup>1</sup>H NMR (500 MHz, CDCl<sub>3</sub>):  $\delta$  4.44 (d, <sup>3</sup>*J* = 5.7 Hz,

(19) Bünzli, J.-C. G.; Piguet, C. *Chem. Soc. Rev.* **2005**, *34*, 1048–1077.

(20) Bünzli, J.-C. G. *Acc. Chem. Res.* **2006**, *39*, 53–61.

(21) Beeby, A.; Bushby, L. M.; Maffeo, D.; Williams, J. A. G. *J. Chem. Soc., Dalton Trans.* **2002**, 48–54.

(22) Werts, M. H. V.; Jukes, R. T. F.; Verhoeven, J. W. *Phys. Chem. Chem. Phys.* **2002**, *4*, 1542–1548.

(23) D'Aléo, A.; Xu, J.; Moore, E. G.; Jocher, C. J.; Raymond, K. N. *Inorg. Chem.* **2008**, *47*, 6109–6111.

(24) Moore, E. G.; Xu, J.; Jocher, C. J.; Werner, E. J.; Raymond, K. N. *J. Am. Chem. Soc.* **2006**, *128*(33), 10648–10649.

(25) Moore, E. G.; Xu, J.; Jocher, C. J.; Castro-Rodriguez, I.; Raymond, K. N. *Inorg. Chem.* **2008**, *47*, 3105–3118.

(26) Kawahara, S.-I.; Uchimaru, T. *Z. Naturforsch. B.* **2000**, *55*, 985–987.

(27) Xu, J.; Durbin, P. W.; Kullgren, B.; Ebbe, S. N.; Uhlir, L. C.; Raymond, K. N. *J. Med. Chem.* **2002**, *45*(18), 3963–3971.

4H), 5.08 (s, 4H), 6.19 (m, 4H), 7.04 (m, 2H), 7.10–7.15 (m, 2H), 7.20–7.40 (m, 12H), 7.83 (m, 2H);  $^{13}\text{C}$  NMR (125 MHz,  $\text{CDCl}_3$ ):  $\delta$  40.5, 78.5, 105.3, 122.5, 127.8, 128.0, 128.7, 129.4, 132.8, 135.0, 142.5, 158.0, 159.9;  $\text{FAB}^+$  MS:  $m/z$ : 590.6 ( $[\text{M} + \text{H}^+]$ ) (calcd: 590.6).

**General Method for the Preparation of 1,2-HOPO Derivatives.** The appropriate 1,2-HOPOBn derivatives were dissolved in concentrated HCl (12 M)/glacial acetic acid (1:1, 20 mL), and were stirred at room temperature for 2 days. Filtration followed by removal of the solvent yielded residues, which were washed with ether to give the deprotected 1,2-HOPO ligands as off-white solids.

**2-Aminomethylaniline-1,2-HOPO ( $\text{L}^2$ ).** Yield: 86%;  $^1\text{H}$  NMR (500 MHz,  $\text{CDCl}_3$ ):  $\delta$  4.49 (s, 2H), 6.36 (d,  $^3J = 7.0$  Hz, 1H), 6.58 (t,  $^3J = 7.5$  Hz, 2H), 6.66 (d,  $^3J = 9.0$  Hz, 1H), 7.26 (t,  $^3J = 7.5$  Hz, 1H), 7.32 (t,  $^3J = 7.5$  Hz, 3H), 7.39–7.52 (m, 4H), 9.28 (t,  $^3J = 6.0$  Hz, 1H), 10.62 (s, 1H);  $^{13}\text{C}$  NMR (125 MHz,  $\text{CDCl}_3$ ):  $\delta$  104.0, 104.5, 119.7, 125.5, 126.4, 127.5, 127.7, 132.6, 134.2, 137.2, 142.1, 157.5, 157.6, 159.2, 160.8;  $\text{FAB}^+$  MS:  $m/z$ : 397.4 ( $[\text{M} + \text{H}^+]$ ) (calcd: 397.4); Anal. Calcd (Found) for  $\text{C}_{19}\text{H}_{16}\text{N}_4\text{O}_6$ : C, 57.58(57.29); H, 4.07(4.01); N, 14.14(13.82).

***o*-Aminomethyl-benzylamine-1,2-HOPO ( $\text{L}^3$ ).** Yield: 90%;  $^1\text{H}$  NMR (500 MHz,  $\text{DMSO}-d_6$ ):  $\delta$  4.50 (d,  $^3J = 6.0$  Hz, 4H), 6.35 (dd,  $^3J = 7.0$  Hz,  $^4J = 1.5$  Hz, 2H), 6.58 (dd,  $^3J = 9.0$  Hz,  $^4J = 1.5$  Hz, 2H), 7.26 (dd,  $^3J = 5.5$  Hz,  $^4J = 2.1$  Hz, 2H), 7.38 (m, 4H), 9.26 (t,  $^3J = 6.0$  Hz, 2H);  $^{13}\text{C}$  NMR (125 MHz,  $\text{DMSO}-d_6$ ):  $\delta$  103.9, 119.6, 127.3, 127.9, 135.9, 137.4, 142.3, 157.6, 160.5;  $\text{FAB}^+$  MS:  $m/z$ : 410.4 ( $[\text{M} + \text{H}^+]$ ) (calcd: 410.4); Anal. Calcd (Found) for  $\text{C}_{19}\text{H}_{16}\text{N}_4\text{O}_6 \cdot \text{MeOH}$ : C, 57.02 (57.01); H, 4.59(5.01); N, 12.88(12.66).

**General Procedure for the Preparation of Lanthanide Complexes.** In a 25 mL round-bottom flask, the appropriate 1,2-HOPO derivative (2 equiv) was suspended in 2 mL of methanol. Gadolinium(III) chloride hexahydrate or europium(III) chloride hexahydrate (1.02 equiv) in 3 mL of methanol and two drops of pyridine were added. The solutions were heated to reflux for 4 h, then cooled to room temperature. Slow evaporation of the methanol at room temperature overnight afforded the desired complexes, as their pyridinium salts, which were collected by filtration.

**Pyridinium[ $\text{Gd}(\text{L}^2)_2$ ].** Yield: 30% (white solid); Anal. Calcd (Found) for  $\text{C}_{43}\text{H}_{34}\text{N}_9\text{O}_{12}\text{Gd} \cdot 4\text{H}_2\text{O}$ : C: 47.03(46.98), H: 3.86(3.73), N: 11.48(11.35); ESI-MS:  $[(\text{GdL}^2)_2]^-$ ;  $m/z$ : 946.1 (calcd: 946.1).

**Pyridinium[ $\text{Eu}(\text{L}^2)_2$ ].** Yield: 35% (white solid); Anal. Calcd (Found) for  $\text{C}_{43}\text{H}_{34}\text{N}_9\text{O}_{12}\text{Eu} \cdot 4\text{H}_2\text{O}$ : C: 47.37(47.26), H: 3.95(3.87), N: 11.41(11.54); ESI-MS:  $[(\text{EuL}^2)_2]^-$ ;  $m/z$ : 941.2 (calcd: 941.10).

**Pyridinium[ $\text{Gd}(\text{L}^3)_2$ ].** Yield: 43% (white solid); Anal. Calcd (Found) for  $\text{C}_{45}\text{H}_{38}\text{N}_9\text{O}_{12}\text{Gd} \cdot 7\text{H}_2\text{O}$ : C: 45.80(46.17), H: 4.44(3.94), N: 10.68(10.49); ESI-MS:  $[(\text{GdL}^3)_2]^-$ ;  $m/z$ : 974.1 (calcd: 974.14).

(28) Frisch, M. J.; Trucks, G. W.; Schlegel, H. B.; Scuseria, G. E.; Robb, M. A.; Cheeseman, J. R.; Montgomery, J. J. A.; Vreven, T. K.; K. N.; Burant, J. C.; Millam, J. M.; Iyengar, S. S.; Tomasi, J.; Barone, V.; Mennucci, B.; Cossi, M.; Scalmani, G.; Rega, N.; Petersson, G. A.; Nakatsuji, H.; Hada, M.; Ehara, M.; Toyota, K.; Fukuda, R.; Hasegawa, J.; Ishida, M.; Nakajima, T.; Honda, Y.; Kitao, O.; Nakai, H.; Klene, M.; Li, X.; Knox, J. E.; Hratchian, H. P.; Cross, J. B.; Bakken, V.; Adamo, C.; Jaramillo, J.; Gomperts, R.; Stratmann, R. E.; Yazyev, O.; Austin, A. J.; Cammi, R.; Pomelli, C.; Ochterski, J. W.; Ayala, P. Y.; Morokuma, K.; Voth, G. A.; Salvador, P.; Dannenberg, J. J.; Zakrzewski, V. G.; Dapprich, S.; Daniels, A. D.; Strain, M. C.; Farkas, O.; Malick, D. K.; Rabuck, A. D.; Raghavachari, K.; Foresman, J. B.; Ortiz, J. V.; Cui, Q.; Baboul, A. G.; Clifford, S.; Cioslowski, J.; Stefanov, B. B.; Liu, G.; Liashenko, A.; Piskorz, P.; Komaromi, I.; Martin, R. L.; Fox, D. J.; Keith, T.; Al-Laham, M. A.; Peng, C. Y.; Nanayakkara, A.; Challacombe, M.; Gill, P. M. W.; Johnson, B.; Chen, W.; Wong, M. W.; Gonzalez, C.; Pople, J. A. *Gaussian 03*, Revision C.02; Gaussian, Inc.: Wallingford, CT, 2004.

**Pyridinium[ $\text{Eu}(\text{L}^3)_2$ ].** Yield: 60% (white solid); Anal. Calcd (Found) for  $\text{C}_{45}\text{H}_{38}\text{N}_9\text{O}_{12}\text{Eu} \cdot 4\text{H}_2\text{O}$ : C: 48.22(48.36), H: 4.14(3.84), N: 11.25(11.11); ESI-MS:  $[(\text{EuL}^3)_2]^-$ ;  $m/z$ : 969.2 (calcd: 969.14).

**Computational Studies.** Ground state density functional theory (DFT) and time-dependent DFT (TD-DFT) calculations were performed at the Molecular Graphics and Computational Facility, College of Chemistry, University of California, Berkeley. In both cases, the B3LYP/6-311G++(d,p) basis set provided in Gaussian<sup>03</sup><sup>28</sup> was used, with simplified input structures derived from a previously reported crystal structure<sup>24,25</sup>. All calculations were done in the gas phase, and geometry optimizations were performed with no symmetry restraints. As a simplified model, only the 6-phenyl amide and 6-benzyl amide of 1,2-HOPO were used as the input structures, and these were first geometry optimized with no symmetry constraints to give the relaxed output geometries.

**Optical Spectroscopy.** UV–visible absorption spectra were recorded on a Varian Cary 300 double beam absorption spectrometer. Emission spectra were acquired on a HORIBA Jobin Yvon IBH FluoroLog-3 spectrofluorimeter, equipped with 3 slit double grating excitation and emission monochromators (2.1 nm/mm dispersion, 1200 grooves/mm). Spectra were reference corrected for both the excitation light source variation (lamp and grating) and the emission spectral response (detector and grating). Luminescence lifetimes were determined on a HORIBA Jobin Yvon IBH FluoroLog-3 spectrofluorimeter, adapted for time-correlated single photon counting (TCSPC) and multi-channel scaling (MCS) measurements. A submicrosecond Xenon flashlamp (Jobin Yvon, 5000XeF) was used as the lightsource, with an input pulse energy (100 nF discharge capacitance) of about 50 mJ, yielding an optical pulse duration of less than 300 ns at fwhm. Spectral selection was achieved by passage through the same double grating excitation monochromator. Emission was monitored perpendicular to the excitation pulse, again with spectral selection achieved by passage through the double grating emission monochromator (2.1 nm/mm dispersion, 1200 grooves/mm). A thermoelectrically cooled single photon detection module (HORIBA Jobin Yvon IBH, TBX-04-D) incorporating fast risetime PMT, wide bandwidth pre-amplifier, and picosecond constant fraction discriminator was used as the detector. Signals were acquired using an IBH DataStation Hub photon counting module, and data analysis was performed using the commercially available DAS 6 decay analysis software package from HORIBA Jobin Yvon IBH. Goodness of fit was assessed by minimizing the reduced chi squared function,  $\chi^2$ , and a visual inspection of the weighted residuals. Each trace contained at least 10,000 points, and the reported lifetime values resulted from at least three independent measurements. Typical sample concentrations for both absorption and fluorescence measurements were about  $10^{-5}$ – $10^{-6}$  M, and 1.0 cm cells in quartz suprasil or equivalent were used for all measurements. Quantum yields were determined by the optically dilute method (with optical density  $< 0.1$ ) using the following equation;

$$\Phi_x/\Phi_r = [Ar(\lambda_r)/Ax(\lambda_x)][I(\lambda_r)/I(\lambda_x)][nx2/nr2][Dx/Dr]$$

where  $A$  is the absorbance at the excitation wavelength ( $\lambda$ ),  $I$  is the intensity of the excitation light at the same wavelength,  $n$  is the refractive index, and  $D$  is the integrated luminescence intensity. The subscripts “x” and “r” refer to the sample and reference, respectively. For quantum yield calculations, an excitation wavelength of 340 nm was utilized for both the reference and sample, hence the  $I(\lambda_r)/I(\lambda_x)$  term is removed. Similarly, the ratio of the refractive indices term,  $nx2/nr2$ , was assumed identical for the aqueous reference and sample solutions. Thus, a plot of integrated emission intensity (i.e.,  $D_r$ ) versus absorbance at 340 nm (i.e.,  $A_r(\lambda_r)$ ) should be linear plot with a slope equal to the reference quantum yield  $\Phi_r$ . Quinine



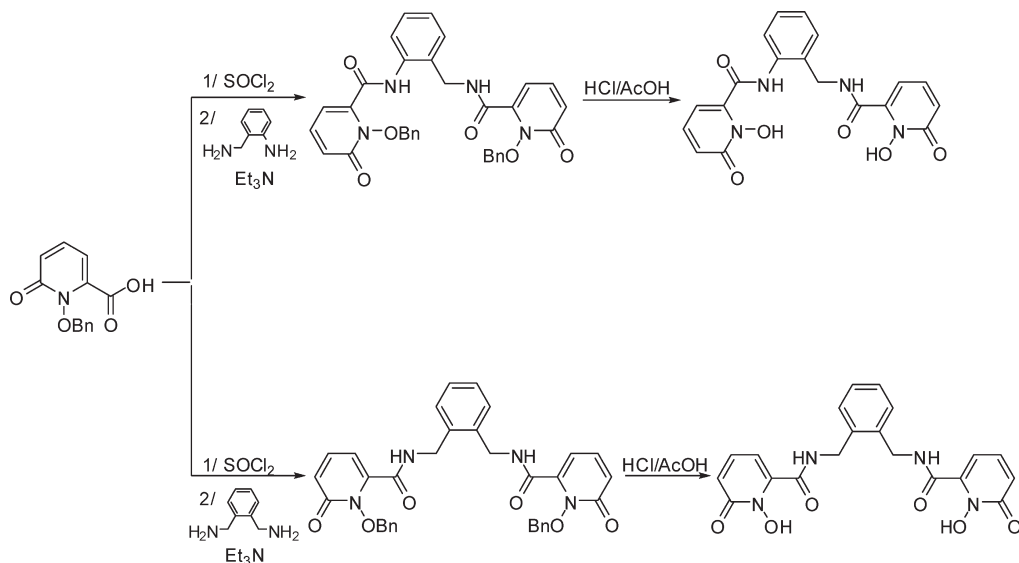


**Figure 1.** Schematic representation of the synthesis pathway.

sulfate in 0.5 M (1.0 N) sulfuric acid was used as the reference ( $\Phi_r = 0.546$ ). A plot of integrated emission intensity for the sample (i.e.,  $Dx$ ) versus absorbance at 340 nm gave the values reported, which are the average of four independent measurements.

## Results and Discussion

**1. Synthesis.** Each of the ligands investigated (Chart 1) incorporates the 1-hydroxypyridin-2-one (1,2-HOPO) group, which acts as a bidentate ligand to complex Ln(III) ions efficiently. The overall tetradentate ligand topology has been shown to form stable  $ML_2$  complexes (where each ligand, L, is a bis-bidentate ligand composed of two such 1,2-HOPO chelates). These units can be linked by aliphatic<sup>24,25</sup> or aromatic spacers<sup>23</sup> (Chart 1) via the amide functional groups. The benzyl protected 1,2-HOPO chromophore (Figure 1) was prepared as reported elsewhere.<sup>29</sup> The acid chloride was prepared in situ by using thionyl chloride,<sup>27</sup> and the resulting intermediate (2.4 equiv) was combined with 1 equiv of the corresponding diamine to furnish the benzyl protected tetradentate ligands. These were boiled in HCl and acetic acid to give the desired ligands in good yields. The Ln(III) complexes (Ln = Eu, Gd) were prepared by heating at reflux 2 equiv of the appropriate ligand with 1 equiv of  $LnCl_3 \cdot 6H_2O$  using pyridine as a base. The product complexes were then precipitated and washed with ether to yield the pure hydrated complexes. X-ray quality crystals of  $[Eu(L^1)_2]^-$  and  $[Eu(L^3)_2]^-$  complex were grown by vapor diffusion of ether into methanol solutions (see ref 23 and Supporting Information, respectively).

**2. Theoretical Calculations.** To obtain a more complete picture of the ligand ground and excited states, TD-DFT calculations using the B3LYP functional were performed using Gaussian'03 following the method of Picard et al.<sup>30</sup> The trivalent Ln cation was substituted by a monovalent

Na atom. For  $L^1$  and  $L^3$  fragments, the resulting optimized geometry and relevant molecular orbital diagrams are depicted in Figure 2, and the resulting predicted electronic transitions in the UV/vis region from TD-DFT analysis summarized in Table 1.

Details of the singlet and triplet state energies can be obtained from these calculations. The  $L^1$  and  $L^3$  linkages are well described by the model presented in Figure 2; the  $L^2$  linkage, with both a phenyl and benzyl linking unit, can be considered as a mixture of both  $L^1$  and  $L^3$ . As noted elsewhere,<sup>25</sup> the calculated lowest unoccupied molecular orbital (LUMO) is metal centered, and transitions involving this orbital (i.e., involving a ligand to metal charge transfer (LMCT) to the Na cation) is an artifact of the underestimate of the lowest energy singlet transition energy.<sup>31</sup> Thus, the orbital labeled LUMO+1 should be considered the LUMO in the case of the Ln(III) complexes. As can be seen from Figure 2, the highest occupied molecular orbital (HOMO)  $\rightarrow$  LUMO+1 transition can be described as a  $\pi-\pi^*$  transition for both systems. Importantly, the second lowest singlet energy (i.e.,  $S_0 \rightarrow S_2$ ) can be described as a combination of the HOMO  $\rightarrow$  LUMO+2 and HOMO-1  $\rightarrow$  LUMO+1 transitions, and these evidently possess some intra ligand charge transfer (ILCT) character. For the  $L^1$  linkage, this ILCT is from the bridge to the central 1,2-HOPO chromophore while for  $L^3$ , the HOMO  $\rightarrow$  LUMO+2 has significant ILCT character from the chromophore to the bridge.

As can also be seen in Tables 1 and 3, the estimated singlet ground state energies and the triplet excited state energies match well with the experimental data. In particular, the triplet excited state is predicted to be near  $21,000\text{ cm}^{-1}$ , in agreement with the previous 1,2-HOPO derivatives already published,<sup>23-25</sup> and is of an energy to efficiently sensitize the europium cation.

**3. UV/visible Absorption Spectroscopy.** The UV/visible absorption data for each of the Eu(III) and Gd(III) complexes in the different solvents are summarized in Table 2 and Figure 3. Each of the spectra have absorption

(29) Scarrow, R. C.; Riley, P. E.; Abu-Dari, K.; White, D. L.; Raymond, K. N. *Inorg. Chem.* **1985**, *24*(6), 954-967.

(30) Gutierrez, F.; Tedeschi, C.; Maron, L.; Daudey, J.-P.; Azema, J.; Tisnès, P.; Picard, C.; Poteau, R. *J. Mol. Struct. Theochem* **2005**, *756*, 151-162.

(31) Dreuw, A.; Head-Gordon, M. *J. Am. Chem. Soc.* **2004**, *126*, 4007-4016.

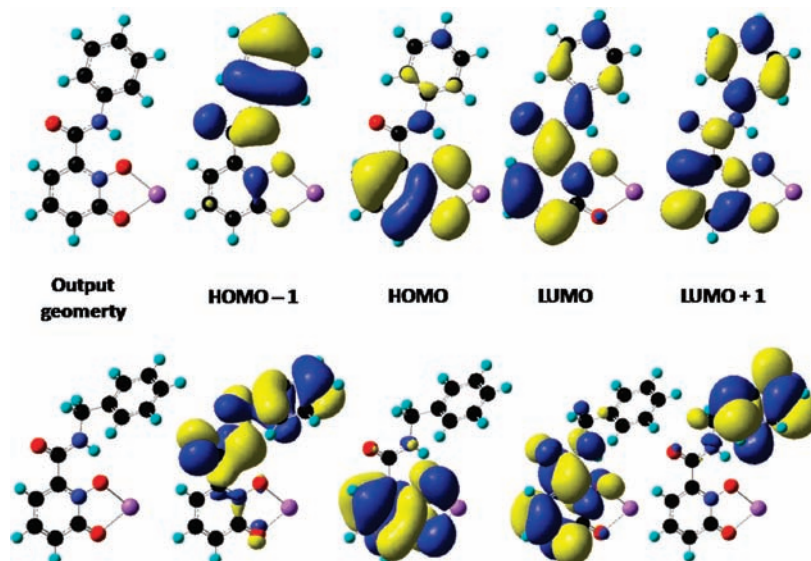


**Figure 2.** Calculated output geometry obtained from static B3LYP/6-311G++ (d,p) geometry optimization and relevant corresponding molecular orbital diagrams from TD-DFT electronic structure calculations for a model  $L^1Na$  (top) and  $L^3Na$  (bottom) complexes.

**Table 1.** UV-visible Absorption Data of Selected Europium Complexes in 0.1 M TRIS Buffered Aqueous Solution (pH = 7.4) and Corresponding Data Calculated for the Model  $Na^+$  Complexes by TD-DFT

	$\lambda_{max}$ (nm)	$\epsilon^{max}$ ( $M^{-1} cm^{-1}$ )	$\lambda_{max}^{calc a}$ (nm)	$f^b$	$\lambda_{max}^{calc c}$ (nm)	assignment
$[Eu(L^1)_2]^-$	342	21,020	345.5	0.64	473.8	HOMO $\rightarrow$ LUMO + 1
$[Eu(L^3)_2]^-$	337	18,690	333.5	0.64	483.2	HOMO $\rightarrow$ LUMO + 1

<sup>a</sup> Wavelength of the lowest-energy singlet absorption band calculated by TD-DFT. <sup>b</sup> Calculated oscillator strength of the pertinent transition. <sup>c</sup> Wavelength of the lowest-energy triplet excited state calculated by TD-DFT.

maxima around 335–340 nm which are composed of two electronic transitions; at lower energy a purely  $\pi-\pi^*$  transition and a slightly higher energy (around ca. 320 nm)  $\pi-\pi^*$  transition with some charge transfer (CT) character, as evidenced by the accompanying TD-DFT calculations (see Figure 2). The absorption maxima follow the expected trend, displaying a red shift with increasing conjugation, going from 336 to 342 nm in buffered aqueous solution for the  $L^3$  and  $L^1$  derivatives respectively. The molar absorption coefficients are within experimental error, with typical values around  $20,000 M^{-1} cm^{-1}$  which is also in agreement with previous results for the aliphatic bridged 1,2-HOPO derivatives.<sup>24,25</sup> Thus, conjugation of a phenyl unit with the 1,2-HOPO chromophore through an amide function does not yield any relevant increase of the molar absorption coefficient. In methanol and DMSO, similar trends in the position of absorption maxima and the value of the molar absorption coefficients were observed.

No differences were observed when comparing the gadolinium and europium complexes, showing the absence of an effect due to the lanthanide cation in the ground state.

**4. Luminescence Properties of the Gadolinium Complexes.** To estimate the energies of the ligand-based triplet excited state, the Gd(III) complexes were studied. Gadolinium is a  $4f^7$  lanthanide cation with a similar metal centered electronic structure and size as the europium cation ( $4f^6$ ), but lacks an accessible metal-based low energy electronic excited state. For these complexes, at room temperature, only a broad weak emission centered

around 400 nm can be seen for  $[Gd(L^2)_2]^-$  and  $[Gd(L^3)_2]^-$  while  $[Gd(L^1)_2]^-$  is almost not emissive (see Supporting Information, Figure S1). This emission can be attributed to the singlet excited state of the 1,2-HOPO chromophore complexed to the gadolinium cation.

At 77 K, in solid matrix, an emission band at about 500 nm can be seen. This emission, red-shifted compared to the singlet excited state, is assigned to the triplet excited state below the singlet excited state observed at room temperature, as illustrated in Figure 4a where the luminescence spectra of the three gadolinium complexes at 77 K are depicted. From these spectra, it appears the triplet excited states of the complexes are located at almost the same energy, varying from 496 to 504 nm for  $[Gd(L^2)_2]^-$  and  $[Gd(L^3)_2]^-$ , respectively. Moreover, this slight shift seems to arise as a result of the differing linewidths of the emission band rather than on any difference in the position of the maxima for the first vibronic transition (see Figure 4a). To confirm that the triplet excited is globally the same for the three complexes, spectral deconvolution of the triplet excited state emission ( $T_{0-0}$ ) into a vibronic progression of several overlapping Gaussian functions with separations of about  $1000-1100 cm^{-1}$  were performed<sup>25,32,33</sup> as presented in Figure 4.

After deconvolution, it was readily apparent that the triplet excited states have almost identical energies,

(32) Jirsakova, V.; Reiss-Husson, F.; Agalidis, I.; Vrieze, J.; Hoff, A. J. *Biochim. Biophys. Acta* **1995**, *1231*, 313–322.

(33) de Weerd, F. L.; Palacios, M. A.; Andrizhiyevskaya, E. G.; Dekker, J. P.; van Grandelle, R. *Biochemistry* **2002**, *41*, 15224–15233.

**Table 2.** UV/visible Absorption of the Eu(III) and Gd(III) Complexes at Room Temperature in Aqueous TRIS, Methanol, and DMSO Solutions

	aqueous TRIS(pH 7.4)		methanol		DMSO	
	$\lambda_{\text{abs}}$ (nm)	$\epsilon$ ( $\text{M}^{-1} \text{cm}^{-1}$ )	$\lambda_{\text{abs}}$ (nm)	$\epsilon$ ( $\text{M}^{-1} \text{cm}^{-1}$ )	$\lambda_{\text{abs}}$ (nm)	$\epsilon$ ( $\text{M}^{-1} \text{cm}^{-1}$ )
[Eu(L <sup>1</sup> ) <sub>2</sub> ] <sup>-</sup>	342 <sup>a</sup>	21,020 <sup>a</sup>	345	21,780	346	20,140
[Gd(L <sup>1</sup> ) <sub>2</sub> ] <sup>-</sup>	342 <sup>a</sup>	21,690 <sup>a</sup>	344	21,110	345	19,830
[Eu(L <sup>2</sup> ) <sub>2</sub> ] <sup>-</sup>	338	20,260	343	21,220	342	20,430
[Gd(L <sup>2</sup> ) <sub>2</sub> ] <sup>-</sup>	339	19,980	344	20,910	342	20,010
[Eu(L <sup>3</sup> ) <sub>2</sub> ] <sup>-</sup>	337	18,690	340	20,640	343	19,980
[Gd(L <sup>3</sup> ) <sub>2</sub> ] <sup>-</sup>	336	19,100	340	20,090	343	19,980

<sup>a</sup> Sample containing 0.3% DMSO (volume).

**Table 3.** Photophysical Data of the Investigated Complexes

	aqueous 0.1 M TRIS (pH = 7.4)				methanol			DMSO		77 K <sup>c</sup>		
	$T_{0-0}$ <sup>b</sup>	$\phi_{\text{Eu}}$	$\tau$ (H) ( $\mu\text{s}$ )	$\tau$ (D) ( $\mu\text{s}$ )	$q$	$\phi_{\text{Eu}}$	$\tau$ (H) ( $\mu\text{s}$ )	$\tau$ (D) ( $\mu\text{s}$ )	$n$	$\phi_{\text{Eu}}$	$\tau$ ( $\mu\text{s}$ )	$\tau$ ( $\mu\text{s}$ )
[Eu(L <sup>1</sup> ) <sub>2</sub> ] <sup>-</sup>	20,964	0.062 <sup>a</sup>	536 <sup>a</sup>	734 <sup>a</sup>	0.2 <sup>a</sup>	0.081	655	748	0.4	0.145	593	734
[Eu(L <sup>2</sup> ) <sub>2</sub> ] <sup>-</sup>	21,230	0.231	567	766	0.1	0.340	623	736	0.5	0.476	740	662
[Eu(L <sup>3</sup> ) <sub>2</sub> ] <sup>-</sup>	20,870	0.051	276	437	1.1	0.188	571	915	1.4	0.319	634	634

<sup>a</sup> Sample containing 0.3% DMSO (volume). <sup>b</sup> Determined using the Gd(III) complex at 77 K in solid matrix (mixture of methanol and ethanol (1:4)). <sup>c</sup> In solid matrix (mixture of methanol and ethanol (1:4)); H represents the hydrogenated solvent while D stand for the deuterated one.

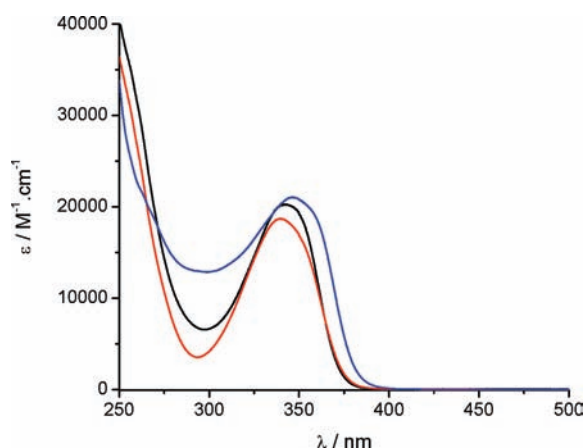


**Figure 3.** UV/visible absorption spectra of [Eu(L<sup>1</sup>)<sub>2</sub>]<sup>-</sup> (red line), [Eu(L<sup>2</sup>)<sub>2</sub>]<sup>-</sup> (black line), and [Eu(L<sup>3</sup>)<sub>2</sub>]<sup>-</sup> (blue line) in 0.1 M TRIS buffered aqueous solution pH = 7.4.

ranging from 20,870  $\text{cm}^{-1}$  to 21,230  $\text{cm}^{-1}$  (Table 3). It is important to note that this energy is ideal, and typical of the 1,2-HOPO chromophore, which, as demonstrated elsewhere, efficiently sensitizes europium luminescence with overall quantum yields on the order of 20%.<sup>24,25</sup>

Noticeably, since the triplet excited state energies of all these ligands are identical, no difference in the energy transfer efficiency is expected, and thus the observed differences in the excited singlet/triplet gap cannot be interpreted with confidence.

### 5. Luminescence Properties of Europium Complexes.

The emission spectra are typical for Eu(III) 1,2-HOPO derivatives, with a very intense  $J = 2$  transition ( ${}^7\text{F}_2 \leftarrow {}^5\text{D}_0$ ) that represents around 84% of the total emission intensities (Figure 5). The spectra also look very similar in different solvents, the only changes observed are with the intensity of the  $J = 1$  band ( ${}^7\text{F}_1 \leftarrow {}^5\text{D}_0$ ) as compared to the overall intensity (Figure 5), yielding different radiative parameters (vide infra).

For the steady state emission spectra, the luminescence quantum yields and luminescence lifetimes of the Eu(III)

complexes were also measured in three different solvents (aqueous with 0.1 M TRIS buffer pH = 7.4, methanol and DMSO solutions) to determine the relevant radiative and non-radiative parameters in these differing environments. Where possible, the luminescence lifetimes were also measured in the corresponding deuterated solvents, to estimate the number of bound solvent molecules in the inner sphere (i.e.,  $q$  in water,<sup>34</sup> and  $n$  in methanol<sup>35</sup>) using the empirical Horrocks equations.

The results presented in Table 3 and 4 show that the bridge has an important influence on all of the various photophysical parameters. For instance, the quantum yields of [Eu(L<sup>1</sup>)<sub>2</sub>]<sup>-</sup> and [Eu(L<sup>3</sup>)<sub>2</sub>]<sup>-</sup> are low compared to that of [Eu(L<sup>2</sup>)<sub>2</sub>]<sup>-</sup> (6.2% and 5.1% vs 23.1%, respectively) in buffered aqueous solution. Furthermore, the luminescence quantum yields in methanol are all higher than the values in water; the quantum yields range from 5% to 23% in buffered aqueous solution (with the best value for [Eu(L<sup>2</sup>)<sub>2</sub>]<sup>-</sup>) and corresponding values as high as 34.0% in methanol. The luminescence lifetimes are also significantly different from each other, which is attributed to the solvation of the complexes in the different media. Estimates of  $q$  reveal the presence of one molecule of water in the inner sphere for [Eu(L<sup>3</sup>)<sub>2</sub>]<sup>-</sup> while, for the other complexes, there are no water molecules in close proximity to the metal. The same trend is observed in methanol, with values around 0.5 and 1.5. These values can be considered as slight overestimates, since the original Horrocks methanol equation does not account for the presence of second sphere solvent molecules nor the quenching effects of proximal N-H vibrations. Importantly, despite a small shift of the triplet excited state, the observed variations in quantum yield and also of luminescence lifetimes are significant, which would not be the case if the sensitization efficiency were only related to the energy of the triplet excited state. Moreover, the obvious

(34) Supkowski, R. M.; Horrocks, W. D. *Inorg. Chim. Acta* **2002**, *340*, 44–48.

(35) Holz, R. C.; Chang, C. A.; Horrocks, W. D. *Inorg. Chem.* **1991**, *30*, 3270–3275.



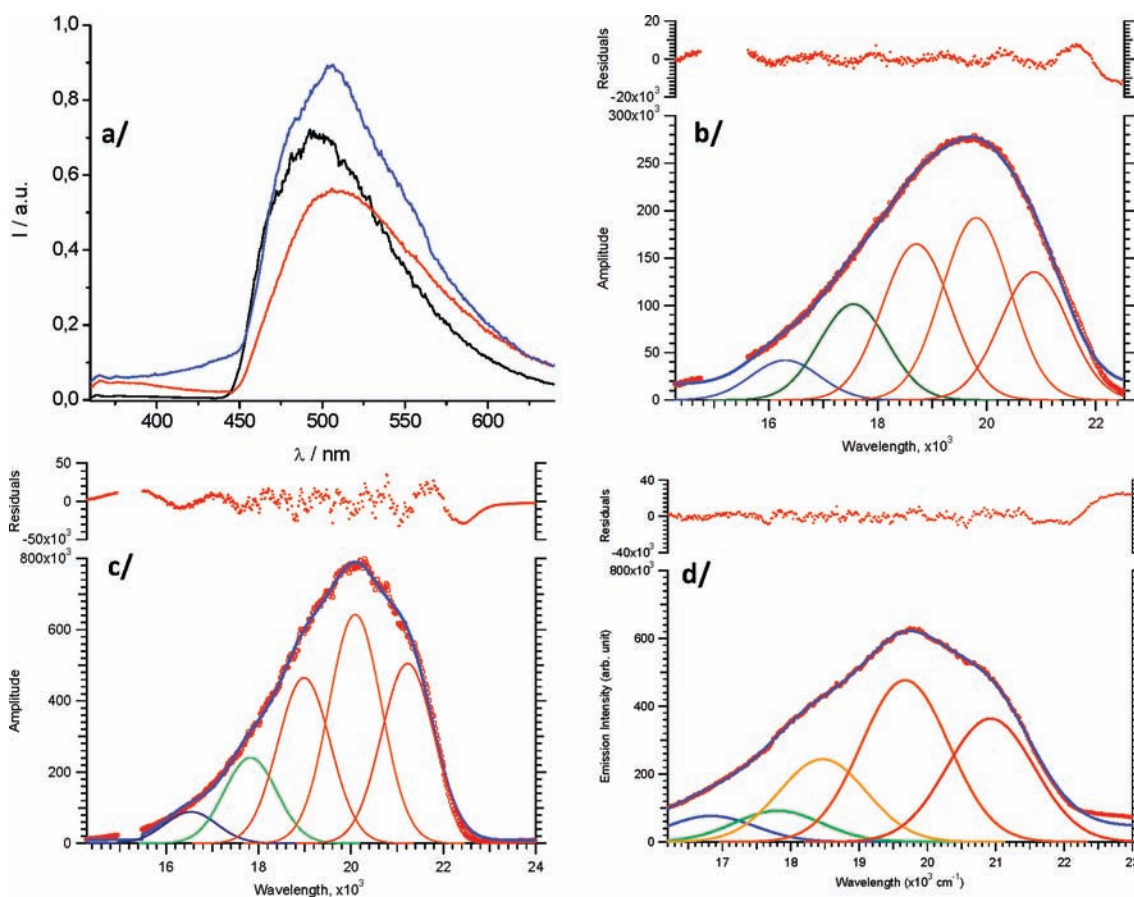


**Figure 4.** Triplet excited state emission from Gadolinium complexes in solid matrix (77 K, methanol/ethanol 1/4) ( $\lambda_{\text{ex}} = 320$  nm): (a)  $[\text{Gd}(\text{L}^1)_2]^-$  (blue line),  $[\text{Gd}(\text{L}^2)_2]^-$  (black line), and  $[\text{Gd}(\text{L}^3)_2]^-$  (red line), (b) deconvolution of  $[\text{Gd}(\text{L}^3)_2]^-$ , (c) deconvolution of  $[\text{Gd}(\text{L}^2)_2]^-$ , and (d) deconvolution of  $[\text{Gd}(\text{L}^1)_2]^-$ .

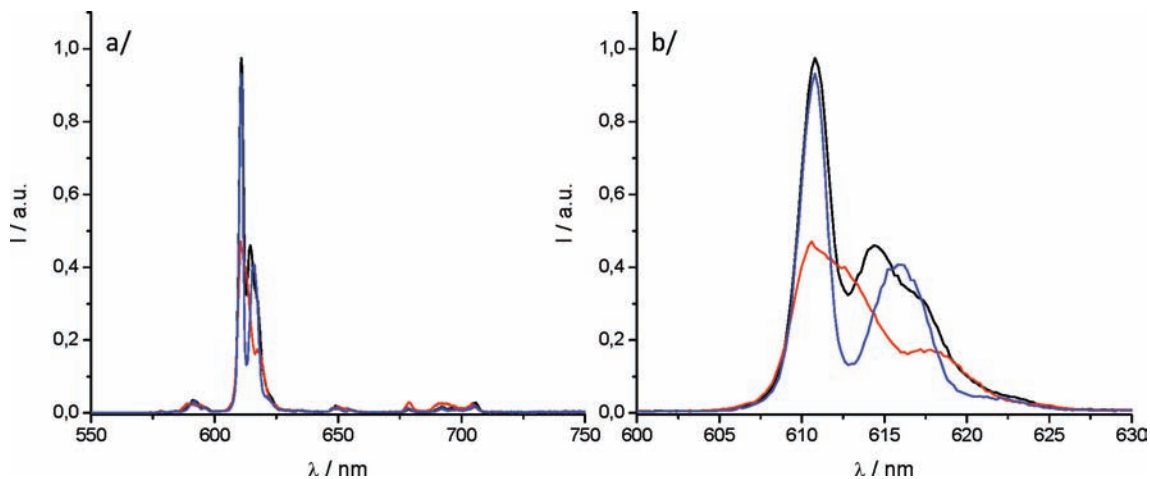


**Figure 5.** Normalized luminescence spectra (on  $J = 1$  transition) of  $[\text{Eu}(\text{L}^1)_2]^-$  (blue line),  $[\text{Eu}(\text{L}^2)_2]^-$  (black line), and  $[\text{Eu}(\text{L}^3)_2]^-$  (red line) in aqueous TRIS solution ( $\lambda_{\text{ex}} = 340$  nm) (a) Full spectra, (b)  $J = 2$  transition.

luminescence quantum yield differences between  $[\text{Eu}(\text{L}^1)_2]^-$  and  $[\text{Eu}(\text{L}^2)_2]^-$  are not accompanied by relevant changes in their luminescence lifetimes. This confirms that, while the triplet excited state energies undoubtedly play an important role in the sensitization process differences, they are not the only critical factor. The geometry of the ligand around the Ln(III) ion induces different intersystem crossing and energy transfer

efficiencies to the Eu(III) cation that also are a crucial factor. The same conclusion can be drawn by comparing  $[\text{Eu}(\text{L}^3)_2]^-$  in non-protic medium to  $[\text{Eu}(\text{L}^2)_2]^-$  and  $[\text{Eu}(\text{L}^1)_2]^-$ .

Luminescence lifetimes were also determined at 77 K, in a solid matrix (Table 3), which allowed determination of whether back energy transfer between the donor triplet excited state and the acceptor manifold excited state of

**Table 4.** Photophysical Data of the Investigated Complexes in Water

complex	solvent	$\phi_{\text{Eu}}$	$\phi_{\text{Eu}}^{\text{theo}}$	$\tau_{\text{Eu}}/\mu\text{s}$	$\tau_{\text{R}}/\mu\text{s}$	$\eta_{\text{Eu}}$	$\eta_{\text{sens}}$	$[I(0,1)/I_{\text{tot}}]$	$k_{\text{R}}/\text{s}^{-1}$	$\Sigma k_{\text{nr}}/\text{s}^{-1}$
[Eu(L <sup>1</sup> ) <sub>2</sub> ] <sup>-</sup>	TRIS	0.062 <sup>a</sup>	0.364 <sup>a</sup>	536 <sup>a</sup>	1470 <sup>a</sup>	0.365 <sup>a</sup>	0.170 <sup>a</sup>	0.0475 <sup>a</sup>	680 <sup>a</sup>	1186 <sup>a</sup>
	MeOH	0.081	0.500	655	1300	0.500	0.162	0.042	764	762
	DMSO	0.145	0.523	593	1134	0.523	0.277	0.050	882	804
[Eu(L <sup>2</sup> ) <sub>2</sub> ] <sup>-</sup>	TRIS	0.231	0.436	567	1300	0.431	0.530	0.042	769	994
	MeOH	0.340	0.488	623	1276	0.488	0.696	0.052	784	821
	DMSO	0.476	0.462	740	1602	0.452	1.030	0.065	624	727
[Eu(L <sup>3</sup> ) <sub>2</sub> ] <sup>-</sup>	TRIS	0.051	0.098	276	1680	0.164	0.522	0.054	595	5494
	MeOH	0.188	0.430	671	1618	0.415	0.430	0.041	618	818
	DMSO	0.319	0.529	634	1386	0.457	0.603	0.061	721	641
[Eu(L <sup>4</sup> ) <sub>2</sub> ] <sup>-</sup>	TRIS	0.207	0.426	737	1728	0.426	0.485	0.056	579	778

<sup>a</sup> Measured adding 0.3% DMSO (volume).

the lanthanide is present, or alternately whether quenching via low lying LMCT state occurs. In either case, luminescence lifetimes would be a few orders of magnitude lower in solution than at 77 K.<sup>36–38</sup>

As can be seen from Table 3 by comparing the 77 K measurements to those in methanol solution, no such quenching occurs since there is only a small difference between the luminescence lifetimes in solution and in solid state (77 K). Hence, we conclude that 1,2-HOPO derivatives possess a triplet state ideally located (around 20,000 and 21,000 cm<sup>-1</sup>) for efficient energy transfer to the europium <sup>5</sup>D<sub>1</sub> level.

**6. Quantitative Determination of the Eu<sup>III</sup> Sensitization Parameters.** Following the work of Beeby et al.<sup>21</sup> and of Verhoeven et al.,<sup>22</sup> the efficiency of the sensitization can be estimated using a method that defines the overall quantum yield of luminescence ( $\phi_{\text{Eu}}$ ) as the product of the efficiency of the intersystem crossing ( $\eta_{\text{ISC}}$ ), the efficiency of the energy transfer ( $\eta_{\text{ET}}$ ) and the efficiency of metal centered luminescence ( $\eta_{\text{Eu}}$ ).

$$\phi_{\text{Eu}} = \eta_{\text{ISC}}\eta_{\text{ET}}\eta_{\text{Eu}} = \eta_{\text{sens}}\eta_{\text{Eu}}$$

In this equation, the  $\eta_{\text{ISC}}$   $\eta_{\text{ET}}$  term cannot be easily broken into its individual components, and the product is instead termed the sensitization efficiency,  $\eta_{\text{sens}}$  ( $\eta_{\text{sens}} = \eta_{\text{ISC}} \eta_{\text{ET}}$ ). The overall quantum yield of luminescence,  $\phi_{\text{Eu}}$ , is determined experimentally while  $\eta_{\text{Eu}}$  is determined as

$$\eta_{\text{Eu}} = \tau_{\text{Eu}}/\tau_{\text{R}}$$

where  $\tau_{\text{Eu}}$  is the measured Eu lifetime and  $\tau_{\text{R}}$  is the pure radiative lifetime that can be estimated from the emission spectra as follows:

$$k_{\text{R}} = 1/\tau_{\text{R}} = A(0,1)[I_{\text{tot}}/I(0,1)]$$

The constant  $A(0,1)$  is the spontaneous emission probability of the <sup>5</sup>D<sub>0</sub>→<sup>7</sup>F<sub>1</sub> transition, equal to 32.4 s<sup>-1</sup> in water and  $I_{\text{tot}}/I(0,1)$  is the ratio of the total integrated emission intensity to the intensity of the <sup>5</sup>D<sub>0</sub>→<sup>7</sup>F<sub>1</sub> transition.

The result of the  $k_{\text{R}}$  can be correlated to the variation of the sum of the non-radiative decay constant:

$$\Sigma k_{\text{nr}} = [(1/\tau_{\text{Eu}}) - k_{\text{R}}]$$

These parameters were calculated for the three complexes in the three different solvents and are reported in Table 4 for aqueous, methanolic, and DMSO solutions, respectively.

As can be seen from Table 4, there are close similarities among the parameter values for the best sensitizers [Eu(L<sup>2</sup>)<sub>2</sub>]<sup>-</sup> and [Eu(L<sup>4</sup>)<sub>2</sub>]<sup>-</sup> (previously reported<sup>24,25</sup>). The slight increase in luminescence quantum yield of [Eu(L<sup>2</sup>)<sub>2</sub>]<sup>-</sup> is due to the efficiency of the sensitization (53.0% vs 48.5%), which leads to increased overall emission quantum yield for [Eu(L<sup>4</sup>)<sub>2</sub>]<sup>-</sup>. For [Eu(L<sup>3</sup>)<sub>2</sub>]<sup>-</sup>, all the parameters related to the europium center ( $\tau_{\text{Eu}}$  and  $\eta_{\text{Eu}}$ ) are very low because of the inner sphere water molecule bound to the metal cation, and hence the non-radiative decay rate is high ( $\Sigma k_{\text{nr}}$ ). Despite this, the sensitization process for [Eu(L<sup>3</sup>)<sub>2</sub>]<sup>-</sup> is almost as good as that of [Eu(L<sup>2</sup>)<sub>2</sub>]<sup>-</sup>. Finally, for [Eu(L<sup>1</sup>)<sub>2</sub>]<sup>-</sup>, the low quantum yield in water can be attributed to an inefficient sensitization process ( $\eta_{\text{sens}} = 17.0\%$ )<sup>39</sup> whereas the remaining parameters are only slightly lower than for [Eu(L<sup>2</sup>)<sub>2</sub>]<sup>-</sup>, which has similar properties in terms of the efficiency of metal centered luminescence.

The analogous study in methanol also reveals that [Eu(L<sup>2</sup>)<sub>2</sub>]<sup>-</sup> possesses optimized parameters for sensitization as in water yielding an overall 48.8% luminescence quantum yield, with an efficiency of sensitization close to 70%. Since methanol also possesses an OH group, the same problem for [Eu(L<sup>3</sup>)<sub>2</sub>]<sup>-</sup> in aqueous solvent can be observed, namely, a residual inner sphere solvent molecule leading to a high non-radiative decay rate constant. Nonetheless, the quantum yield is good (18.8%) considering the presence of a molecule of methanol in the inner sphere. Here again, the limiting factor is based on the metal's intrinsic luminescence properties. For [Eu(L<sup>1</sup>)<sub>2</sub>]<sup>-</sup>, as in water, the sensitization efficiency is the limiting factor (16.2%). Notably, the luminescence quantum yield in methanol is higher for [Eu(L<sup>3</sup>)<sub>2</sub>]<sup>-</sup> than for [Eu(L<sup>1</sup>)<sub>2</sub>]<sup>-</sup> proving that the sensitization efficiency is more important than the presence of a solvent molecule in such solvent.

Lastly, since DMSO is a non protic solvent, this removes the effect of the OH vibration on the metal luminescence. As can be seen from Table 4, in DMSO, [Eu(L<sup>3</sup>)<sub>2</sub>]<sup>-</sup> has an impressive luminescence quantum yield (31.9%) with an efficient sensitization process (60.3%) and a europium efficiency (45.7%) close to the one

(36) Zucchi, G.; Ferrand, A.-C.; Scopelliti, R.; Bünzli, J.-C. G. *Inorg. Chem.* **2002**, *41*(9), 2459–2465.

(37) Katagiri, S.; Hasegawa, Y.; Wada, Y.; Yanagida, S. *Chem. Lett.* **2004**, *33*(11), 1438–1439.

(38) Joher, C. J.; Moore, E. G.; Pierce, J. D.; Raymond, K. N. *Inorg. Chem.* **2008**, *47*(18), 7951–7953.

(39) We determined that inefficient sensitization arises from the fast non-radiative decay from the singlet or triplet excited states rather than from oxygen quenching because luminescence properties were unchanged upon degassing the solutions.



obtained for our best Eu complex. It is also worth pointing out the 100% efficiency of the sensitization process for  $[\text{Eu}(\text{L}^2)_2]^-$  in DMSO, which shows that the sensitization within the system is almost fully optimized, with a luminescence quantum yield of 47.6%. By contrast, for  $[\text{Eu}(\text{L}^1)_2]^-$ , the same problem of inefficient sensitization can be observed in DMSO, demonstrating that the bridge (and geometry change) in this case influences the sensitization process more than the metal related parameters.

### Conclusion

In conclusion, the Eu(III) HOPO complexes are promising for time-resolved luminescence application. To see the effect of geometry and electronic properties of the bridge on the optical properties, three complexes containing 1,2-HOPO derivatives bridged by aromatic units have been prepared and studied. The photophysical properties of the Gd(III) and Eu(III) complexes have been evaluated together with supporting TD-DFT calculations for the ligand in a model compound. Upon sensitization of the Eu(III) cation, these three systems behave quite differently for reasons which are not related to the triplet excited state energies. While one acts as an efficient europium sensitizer ( $(\text{L}^2)$ , 23.1% luminescence quantum yield in 0.1 M TRIS aqueous solution), the two other systems give poor sensitization, for different reasons: for  $[\text{Eu}(\text{L}^3)_2]^-$ , the low quantum yield and luminescence

lifetime are due to the presence of a water molecule bound in the inner sphere of the metal center (i.e., low values of all parameters related to the europium center), while for  $[\text{Eu}(\text{L}^1)_2]^-$ , the low emission quantum yield is mainly due to an inefficient sensitization process (i.e., intersystem crossing, energy transfer, or both phenomena). To conclude, these three different complexes illustrate the effect of coordinated ligand geometry on the antenna properties that result in different sensitization and/or metal-centered luminescent properties. The use of such a bridge allows one to obtain bright Eu(III) complexes (23.1%), but the geometry around the metal can also yield a poor sensitization efficiency. Work toward better understanding this sensitization process is currently in progress in our group.

**Acknowledgment.** This work was partially supported by the NIH (Grant HL69832) and supported by the Director, Office of Science, Office of Basic Energy Sciences, and the Division of Chemical Sciences, Geosciences, and Biosciences of the U.S. Department of Energy at LBNL under Contract No. DE-AC02-05CH11231. This technology is licensed to Lumiphore, Inc. in which some of the authors have a financial interest.

**Supporting Information Available:** Additional information as noted in the text. This material is available free of charge via the Internet at <http://pubs.acs.org>.